# Anisotropic damping of the magnetization dynamics in Fe, Ni and Co

Daniel Steiauf, Jonas Seib, and Manfred Fähnle*

*Max-Planck-Institut für Metallforschung,*

*Heisenbergstraße 3, 70569 Stuttgart, Germany*

Keith Gilmore and M. D. Stiles

*National Institute of Standards and Technology,*

*Center for Nanoscale Science and Technology,*

*Gaithersburg, Maryland 20899-6202, USA*

(Dated: August 20, 2009)

## Abstract

The Gilbert parameter $\alpha$ describing the damping of magnetization dynamics is commonly taken to be an isotropic scalar. We argue that it is a tensor $\underline{\underline{\alpha}}$ that is anisotropic, leading to a dependence of the damping on both the instantaneous direction of the magnetization $\mathbf{M}(t)$ (orientational anisotropy) and on the direction of rotation of the magnetization (rotational anisotropy). For small-angle precession of $\mathbf{M}$ around a prescribed axis in the crystal, the rotational anisotropy is averaged out and the damping is determined by an effective damping scalar $\alpha_{\mathrm{eff}}$ which depends on the orientation of the prescribed axis. The quantity $\alpha_{\mathrm{eff}}$ of Fe, Ni and Co is calculated for various orientations as a function of the electronic scattering rate. The calculations are performed by the ab-initio density functional electron theory within the framework of the torque-correlation model. The intraband contribution of this model (breathing Fermi surface contribution) is anisotropic for all scattering rates. In contrast, the interband contribution (bubbling Fermi surface contribution) is anisotropic only at small scattering rate ($\tau^{-1}$), but becomes increasingly isotropic as $\tau^{-1}$ increases. Because the latter contribution dominates at high $\tau^{-1}$, each material should exhibit isotropic damping at sufficiently high $\tau^{-1}$ (i.e., sufficiently high temperatures).

PACS numbers: 75.40.Gb, 76.60.Es, 76.50.+G

## I. INTRODUCTION

In recent years there has been a steadily growing interest in fast magnetization dynamics on time scales between several picoseconds and nanoseconds, especially for micro- and nanosized magnets because of their potential use in advanced information storage and data processing devices. Examples are the dynamics of domain walls in nanowires[1], the magnetization reversal in nanomagnets[1] and the dynamics of vortices[2]. From a theoretical point of view, most investigations have been simulations based on Gilbert's equation of motion[3] for the magnetization $\mathbf{M}(\mathbf{r},t)$,

$$\frac{\mathrm{d}\mathbf{M}}{\mathrm{d}t} = -\gamma(\mathbf{M}\times\mathbf{H}_{\mathrm{eff}}) + \frac{1}{M}\mathbf{M}\times\alpha\frac{\mathrm{d}\mathbf{M}}{\mathrm{d}t}\,, \tag{1}$$

or on extensions of this equation including the effect of spin-polarized transport currents. In Eq. (1) the first term describes the precession around an effective field $\mathbf{H}_{\mathrm{eff}}$ ($\gamma$ is the gyromagnetic ratio). The second term describes the damping, i.e., the relaxation of the magnetization direction toward the equilibrium orientation parallel to $\mathbf{H}_{\mathrm{eff}}$, and $\alpha$ is the damping scalar which is typically treated as a scalar constant.

More recently, various theoretical approaches have suggested that for a more realistic description of the magnetization dynamics Gilbert's damping term should be replaced by a more complicated form. For instance, the damping scalar $\alpha$ has been replaced[4–11] by a damping matrix $\underline{\underline{\alpha}}$. This represents a first type of anisotropy of the damping, because it means that the damping is different for different directions of the change $\mathrm{d}\mathbf{M}/\mathrm{d}t$ of the magnetization (rotational anisotropy). Furthermore, it has been proposed[5,7–11] that $\underline{\underline{\alpha}}$ depends on the momentary configuration $\mathbf{M}(\mathbf{r},t)$. For the case of a collinear system, e.g., this represents a second type of anisotropy (orientational anisotropy) because the damping depends on the momentary orientation of $\mathbf{M}(t)$. Finally, it has been noted[6,8] that in general, e.g., for a noncollinear configuration $\mathbf{M}(\mathbf{r},t)$, the damping matrix is nonlocal, i.e., it relates the time-derivative $\mathrm{d}\mathbf{M}(\mathbf{r},t)/\mathrm{d}t$ at site $\mathbf{r}$ to the derivatives $\mathrm{d}\mathbf{M}(\mathbf{r}',t)/\mathrm{d}t$ at other sites $\mathbf{r}'$.

The rotational anisotropy is related to the fact that the damping matrix has two nonzero eigenvalues which are different for an arbitrary orientation of the magnetization in the crystal, and because of the orientational anisotropy both eigenvalues depend on this orientation. For a magnetization direction which corresponds to a three- or fourfold symmetry direction of the crystal the two eigenvalues are the same, i.e., there is no rotational anisotropy. In a

ferromagnetic resonance experiment, the strong external dc field selects a crystal orientation about which the magnetization vector precesses under the action of an additional small perpendicular ac field. It has been shown[11] that under these circumstances the rotational anisotropy is averaged out: The FMR linewidth is to a very good approximation described by an effective damping scalar $\alpha_{\text{eff}}$ which is just the arithmetic mean of the two eigenvalues for the magnetization direction prescribed by the dc field. Because of the orientational anisotropy of the two eigenvalues, $\alpha_{\text{eff}}$ depends on the orientation of the dc field.

In the present paper we consider the temperature dependence of the anisotropy of $\alpha_{\text{eff}}$. The anisotropy and its temperature dependence will be different for different physical processes leading to damping (a review on different damping mechanisms is given in Ref. 12). We confine ourselves to the damping due to the creation of electron-hole pairs resulting from time-dependent spin-orbit interactions and their subsequent relaxation via scattering at phonons or lattice defects. This process is the dominant damping mechanism in metallic ferromagnets. The theoretical approaches to describe this mechanism may be subdivided into two categories: In the first category the damping parameter is determined from the low-frequency limit of the transverse-spin-response function which is calculated using model Hamiltonians[13,14] or time-dependent spin-density-functional electron theory[15]. In the second category[7,8,16,17] an effective field for the magnetization dynamics is defined as the variation of the electronic energy with respect to the magnetization direction, $\delta E/\delta \mathbf{M}$. In a static situation this effective field is equivalent to the magnetocrystalline anisotropy field, whereas in a nonadiabatic dynamical situation irreversible contributions appear which give rise to damping. The relation between these two approaches is discussed in Refs. 17 and 18. It is common to all these approaches that the creation of electron-hole pairs is treated explicitly whereas the subsequent relaxation due to scattering at phonons or defects is accounted for just phenomenologically by a finite lifetime $\tau$ of the states entering the electron spectral functions[14,15,17–19] or by a relaxation time for the nonequilibrium occupation numbers for the electronic states. As a result, the calculated damping contains the lifetime or the relaxation time as open parameter and can be compared quantitatively with experimental results only when inserting some estimate for these quantities (e.g., from conductivity measurements).

The above mentioned theories have shown that there are two contributions to damping originating from the creation of electron-hole pairs, one which is proportional to the electrical conductivity that decreases with temperature and one which is proportional to the resistivity

which increases with temperature. In case of Ni these two contributions have been resolved very clearly in the experiments[20]. For the first contribution a generalized Gilbert equation could be derived (see above) from an effective field approach[7,8] for a general trajectory of $\mathbf{M}(t)$ in which the constant Gilbert scalar $\alpha$ is replaced by a matrix $\underline{\underline{\alpha}}(\mathbf{M}(t))$ so that both the rotational and orientational damping anisotropy are included. The calculations for the second contribution[13–15,17,19] consider from the very beginning the reaction of the system for a special trajectory of $\mathbf{M}(t)$, i.e., for the small-angle precession of $\mathbf{M}(t)$ around a prescribed direction, like in a FMR experiment, i.e., they yield the effective damping scalar $\alpha_{\text{eff}}$ for that prescribed direction. In the present paper both the conductivity-like and the resistivity-like contribution to $\alpha_{\text{eff}}$ are calculated. The purpose of this work is to compare the anisotropies of these two contributions as functions of the scattering rate of the electrons in order to quantify the validity of neglecting this effect in the analysis of experimental results.

## II. DAMPING DUE TO THE CREATION OF ELECTRON-HOLE PAIRS

In some of the formal derivations of the equations for damping the physics underlying the conductivity-like and the resistivity-like contributions is hard to recognize. Therefore, the two contributions have been illuminated more clearly by rederiving them from approaches which are designed in such a way that the underlying physics becomes more apparent[17,18]. Before presenting the numerical results of these calculations we want to approach the two contributions from a further and alternative viewpoint, hoping that this leads to an even more improved understanding of the physics of damping. Both contributions are related to the generation of electron-hole pairs by the magnetization dynamics. The subsequent relaxation of the excited electrons and the holes by scattering at phonons or lattice defects in general will transfer angular momentum from the spin system to the lattice, and this is responsible for the damping of the magnetization dynamics. We focus on the physics behind the generation of the electron-hole pairs; the scattering is accounted for phenomenologically via a relaxation time $\tau$.

In the following we consider a situation for which the micromagnetic magnetization entering Eq. (1) is homogeneous, i.e., $\mathbf{M}(\mathbf{r},t) = \mathbf{M}(t) = M\mathbf{e}(t)$. Furthermore, we are only interested in the temporal evolution of the system on the time scale of ns to several ps. Then $\mathbf{M}(t)$ may be obtained from the microscopic spin magnetization density $\mathbf{m}(\mathbf{r},t)$ by a

coarsegraining procedure[21],

$$\mathbf{M}(t) = M\mathbf{e}(t) = \frac{1}{\Omega}\frac{\nu}{2}\int_{\Omega} \mathrm{d}^3 r \int_{t-1/\nu}^{t+1/\nu} \mathrm{d}t' \mathbf{m}(\mathbf{r}, t') \tag{2}$$

where $\Omega$ is the volume of the sample and where the integration in time averages over the fast magnetic degrees of freedom, i.e., over the fluctuations on a time scale shorter than the inverse of the frequency $\nu$ of a typical long-wavelength spin wave.

For a complete quantum mechanical description of magnetization dissipation, i.e., of the transfer of angular momentum and energy from the electronic system to the lattice, one must start from the time-dependent wave equation for electrons and nuclei, involving spin-orbit coupling which mediates this transfer. Instead, we will describe the situation by an effective single-electron theory that involves only electrons and holes and that describes the transfer via scattering of electrons or holes which is accounted for phenomenologically by the aforementioned lifetime (relaxation time) $\tau$.

We want to approach the problem from two opposing limits, i.e., $\tau \to 0$ and $\tau \to \infty$. In the first case (strictly adiabatic situation) the electronic scattering processes are so frequent that the electronic system is always in its ground state with respect to the momentary orientation $\mathbf{e}(t)$ which can be considered as an external parameter. Then we can define (e.g., by the solution of the Kohn-Sham equations of the density functional electron theory for prescribed $\mathbf{e}(t)$) adiabatic single-electron energies $\varepsilon_{j\mathbf{k}}(\mathbf{e}(t))$ where $j$ and $\mathbf{k}$ denote the band index and the wavevector, the corresponding wavefunctions $|\Psi_{j\mathbf{k}}(\mathbf{e}(t))\rangle$, the adiabatic Fermi-Dirac occupation numbers $f_{j\mathbf{k}}(\mathbf{e}(t))$ and the adiabatic Fermi surface $S(\mathbf{e}(t))$. Because of the action of the spin-orbit coupling, all these quantities change in time when $\mathbf{e}$ changes in time, i.e., the Fermi surface will continuously attain a slightly different form (breathing Fermi surface Fig. 1a). It can be shown by quantum mechanical arguments[21] that in the strictly adiabatic situation there is no damping at all.

For the opposing case, $\tau \to \infty$, there are no scattering processes at all and hence again no damping. The many-electron wavefunction $\Psi(s_1, s_2, \ldots s_N, t)$ for the $N$ electrons then evolves in time coherently according to the time-dependent Schrödinger equation. As initial condition $\Psi(s_1, s_2, \ldots s_N, t = 0)$ we can use, e.g., the adiabatic many-electron wavefunction for an initial orientation $\mathbf{e}(t = 0)$ which does not correspond to a high-symmetry direction of the crystal. From $\Psi(s_1, s_2, \ldots s_N, t)$ we can calculate the microscopic spin-magnetization $\mathbf{m}(\mathbf{r}, t)$, from which the momentary $\mathbf{e}(t)$ are obtained by use of Eq. (2). From the solu-

tion of the Kohn-Sham equations for this $\mathbf{e}(t)$ the adiabatic quantities $\varepsilon_{j\mathbf{k}}(\mathbf{e}(t))$, $\Psi_{j\mathbf{k}}(\mathbf{e}(t))$, $f_{j\mathbf{k}}(\mathbf{e}(t))$ and $S(\mathbf{e}(t))$ are determined. Finally, we can represent the many electron wavefunction $\Psi(s_1, s_2, \ldots s_N, t)$ by the adiabatic single-electron wavefunctions $\Psi_{j\mathbf{k}}(\mathbf{e}(t))$. The occupation numbers $n_{j\mathbf{k}}(t) = \langle\Psi(s_1, s_2, \ldots s_N, t)|\, \hat{a}^\dagger_{\mathbf{k}j}\hat{a}_{\mathbf{k}j}\, |\Psi(s_1, s_2, \ldots s_N, t)\rangle$, where $\hat{a}^\dagger_{\mathbf{k}j}\hat{a}_{\mathbf{k}j}$ is the particle number operator for the single-electron state $(j\mathbf{k})$, in general will be different from the adiabatic occupation numbers $f_{j\mathbf{k}}(\mathbf{e}(t))$. This occurs because without scattering the electronic system will be driven away from the adiabatic situation, i.e., there will be a generation of excited electrons and holes when we consider the strictly adiabatic situation as the corresponding momentary reference situation.

In a realistic situation there are scattering processes which require a finite time (i.e., $\tau$ is nonzero and finite) and which tend to drive the occupation numbers $n_{j\mathbf{k}}(t)$ toward the adiabatic occupation numbers $f_{j\mathbf{k}}(t)$ by a relaxation of the electron-hole pairs. We thereby can distinguish between pairs for which the electrons and holes appear in the same adiabatic band, respectively, and pairs for which electrons and holes are generated by transitions between different bands. To illustrate the physical reason for the generation of these two types of pairs it is convenient to consider the situation from the viewpoint of the hypothetical adiabatic reference situation. The first type is generated because the spin orbit energy of each adiabatic single electron state changes when $\mathbf{e}(t)$ varies in time. Some states which were just below the Fermi surface for time $t-\mathrm{d}t$ get pushed above the Fermi surface for time $t$, whereas other states which were originally above are pushed below. For very frequent scattering processes the real many-electron wavefunction would evolve adiabatically, i.e., $n_{j\mathbf{k}}(t) = f_{j\mathbf{k}}(t)$, and there would be no damping at all (see above). For finite $\tau$, however, the actual occupation numbers $n_{j\mathbf{k}}(t)$ lag behind the adiabatic occupation numbers $f_{j\mathbf{k}}(t)$. Therefore it may be that at time $t$ some of the adiabatic states which were originally occupied at time $t - \mathrm{d}t$ and which would be empty in an adiabatic situation are still occupied, whereas some other states which should be occupied are still empty (Fig. 1b). The intraband relaxation of these electron-hole pairs leads to the transfer of angular momentum from the spin system to the lattice. This so-called intraband or *breathing Fermi surface contribution*[7,8,16–19] to damping increases linearly with $\tau$ and thus represents the conductivity-like term. The second type of pairs is generated because the system of adiabatic single-electron wavefunctions $\Psi_{j\mathbf{k}}$ feels a time-dependent perturbation due to the changing spin-orbit interaction, and this leads to band transitions between the adiabatic states $\Psi_{j\mathbf{k}}(\mathbf{e}(t))$ and $\Psi_{j'\mathbf{k}}(\mathbf{e}(t))$ (The initial

and final states have the same wavevector $\mathbf{k}$ because the transitions are caused by the uniform mode $\mathbf{e}(t)$ which has a wavevector of zero.). Thereby, the number of final states accessible by the perturbation increases with decreasing $\tau$ due to the lifetime broadening of the states (Fig. 1b), and it turns out that this so-called[17] interband or *bubbling Fermi surface contribution* to damping increases monotonically with $1/\tau$ and hence represents the resistivity-like term. It has been shown in Refs. 17,18 that the breathing and the bubbling Fermi surface contributions obtained from the physical reasonings of this paragraph are identical to the intraband and interband contributions of Kamberský's torque correlation model[14].

## III. RESULTS FOR THE ANISOTROPY OF THE EFFECTIVE DAMPING CONSTANT $\alpha_{\text{eff}}$

Figure 2 shows results for Fe, Ni and Co for the effective damping constant $\alpha_{\text{eff}}$ as a function of the inverse lifetime $\tau^{-1}$ for various directions of the prescribed axis around which the magnetization vector precesses. As discussed in section I, for the high-symmetry directions (which are $\langle 001 \rangle$ and $\langle 111 \rangle$ in Fe and Ni, and $\langle 0001 \rangle$ in Co) the two eigenvalues of the damping matrix are the same and thus $\alpha_{\text{eff}}$ is identical to that eigenvalue. We present the total, intraband, and interband contribution of Kamberský's torque correlation model as calculated by the linear augmented plane wave method in the local spin density approximation (details of the calculation are given in Ref. 18). It becomes obvious from Fig. 2 that for small $\tau^{-1}$ the conductivity-like contribution dominates whereas for increasing temperature the resistivity-like contribution takes over, so that the damping exhibits a minimum. Whatever the relation $\tau(T)$, the calculated minimum can be compared directly and quantitatively with the experimentally measured minimum. It has been shown in Ref. 18 that for Fe $\langle 001 \rangle$ and Ni $\langle 111 \rangle$ these two values agree rather well, demonstrating that the torque correlation model accounts for the dominant contribution to damping in these systems. The present objective is to compare the orientational anisotropy of $\alpha_{\text{eff}}$ of the intra- and interband contributions. Since the electron scattering rate $\tau^{-1}$ increases with the number of thermally excited phonons, the results give a qualitative sense for the temperature dependence of the anisotropy of the damping.

Calculations of $\alpha_{\text{eff}}$ were performed for a number of orientations, but for the purposes of

clarity results for only a few of these orientations are presented in Fig. 2. The present findings corroborate previous work that investigated the orientational anisotropy of the eigenvalues of the conductivity-like contribution to the damping parameter. We find here that the orientational anisotropy present in these eigenvalues is maintained in the conductivity-like contribution of the rotationally averaged $\alpha_{\text{eff}}$ and that this anisotropy persists for all $\tau^{-1}$. The conductivity-like contribution to $\alpha_{\text{eff}}$ for all directions tested in Fe and Ni was bounded by the values for the high-symmetry directions, while for Co the high-symmetry direction yielded the minimal $\alpha_{\text{eff}}$ of all orientations tested.

While the conductivity-like contribution is anisotropic for all $\tau^{-1}$, the anisotropy of the resistivity-like contribution decreases with increasing $\tau^{-1}$ (i.e., with increasing temperature). Anisotropy of the resistivity-like contribution arises when the number of interband transitions that occur for a given lifetime broadening of the states is different for the bandstructure belonging to one orientation than for the bandstructure belonging to another orientation. When the lifetime broadening is much larger than the energy differences that occur when switching between orientations, then equally many transitions are allowed for the different orientations, i.e., the damping becomes isotropic.

## IV. CONCLUSIONS

To conclude, we have shown that the conductivity-like contribution to magnetization damping is anisotropic for all scattering rates $\tau^{-1}$ whereas the anisotropy of the resistivity-like contribution decreases with increasing $\tau^{-1}$. The anisotropy of the resistivity-like contribution decreases as the thermal energy becomes comparable to the spin-orbit energy. Therefore, any system will exhibit an isotropic damping at sufficiently high scattering rates. Whether intrinsic damping is isotropic at room temperature depends on the details of the band structure and the strength of the spin-orbit coupling of the material under consideration. For Ni (for which both the conductivity-like and the resistivity-like contribution could be resolved experimentally[20]) an anisotropy of the linewidth of ferromagnetic resonance FMR has been observed for low temperatures, giving a hint to anisotropic damping, whereas other materials did not show a clear indication for an anisotropic intrinsic FMR linewidth (see Ref. 11 and Refs. therein). We suspect that the anisotropy of $\alpha_{\text{eff}}$ would be more prominent in systems with stronger spin-orbit coupling, such as magnetic semiconductors.

* faehnle@mf.mpg.de

[1] M. Kläui and C. A. F. Vaz, in *Handbook of Magnetism and Advanced Magnetic Materials*, edited by H. Kronmüller and S. Parkin (Wiley, New York, 2007), Vol. 2, p. 879; L. Thomas and S. Parkin, in *Handbook of Magnetism and Advanced Magnetic Materials*, edited by H. Kronmüller and S. Parkin (Wiley, New York, 2007), Vol. 2, p. 942.

[2] B. Van Waeyenberge, A. Puzic, H. Stoll, K. W. Chou, T. Tyliszczak, R. Hertel, M. Fähnle, H. Brückl, K. Rott, G. Reiss, I. Neudecker, D. Weiss, C. H. Back, and G. Schütz, Nature **444**, 503 (2006); M. Curcic, B. Van Waeyenberge, A. Vansteenkiste, M. Weigand, V. Sackmann, H. Stoll, M. Fähnle, T. Tyliszczak, G. Woltersdorf, C. H. Back, and G. Schütz, Phys. Rev. Lett. **101**, 197204 (2008); S. Bohlens, B. Krüger, A. Dreuss, M. Bolte, G. Meier, and D. Pfannkuche, Appl. Phys. Lett. **93**, 142508 (2008).

[3] T. L. Gilbert, Ph.D. thesis, Illinois Institute of Technology, 1956.

[4] V. L. Safonov and H. N. Bertram, Phys. Rev. B **71**, 224402 (2005).

[5] K. Capelle and B. L. Gyorffy, Europhys. Lett. **61**, 354 (2003).

[6] T. L. Gilbert, IEEE Trans. Magn. **40**, 3443 (2004).

[7] J. Kuneš and V. Kamberský, Phys. Rev. B **65**, 212411 (2002); **68**, 019901(E) (2003).

[8] D. Steiauf and M. Fähnle, Phys. Rev. B **72**, 064450 (2005); M. Fähnle, D. Steiauf, and J. Seib, J. Phys. D **41**, 164014 (2008); D. Steiauf, J. Seib, and M. Fähnle, Phys. Rev. B **78**, 020410(R) (2008); J. Seib, D. Steiauf, and M. Fähnle, Phys. Rev. B **79**, 064419 (2009).

[9] A. Brataas, Y. Tserkovnyak, and G. E. W. Bauer, Phys. Rev. Lett. **101**, 037207 (2008).

[10] S. Zhang and S. S. L. Zhang, Phys. Rev. Lett. **102**, 086601 (2009).

[11] J. Seib, D. Steiauf, and M. Fähnle, Phys. Rev. B **79**, 092418 (2009).

[12] B. Heinrich, *Ultrathin Magnetic Structures III* (Springer, New York, 2005).

[13] V. Korenman and R.E. Prange, Phys. Rev. B **6**, 2769 (1972).

[14] V. Kamberský, Czech. J. Phys., Sect. B **26**, 1366 (1976).

[15] I. Garate and A. MacDonald, Phys. Rev. B **79**, 064403 (2009).

[16] V. Kamberský, Can. J. Phys. **48**, 2906 (1970).

[17] K. Gilmore, Y. U. Idzerda, and M. D. Stiles, J. Appl. Phys. **103**, 07D303 (2008).

[18] K. Gilmore, Y. U. Idzerda, and M. D. Stiles, Phys. Rev. Lett. **99**, 027204 (2007).

[19] V. Kamberský, Phys. Rev. B **76**, 134416 (2007).

[20] B. Heinrich, D. J. Meredith, and J. F. Cochrane, J. Appl. Phys. **50**, 7726 (1979).

[21] M. Fähnle and D. Steiauf, in *Handbook of Magnetism and Advanced Magnetic Materials*, edited by H. Kronmüller and S. Parkin (Wiley, New York, 2007), Vol. 1, p. 282.

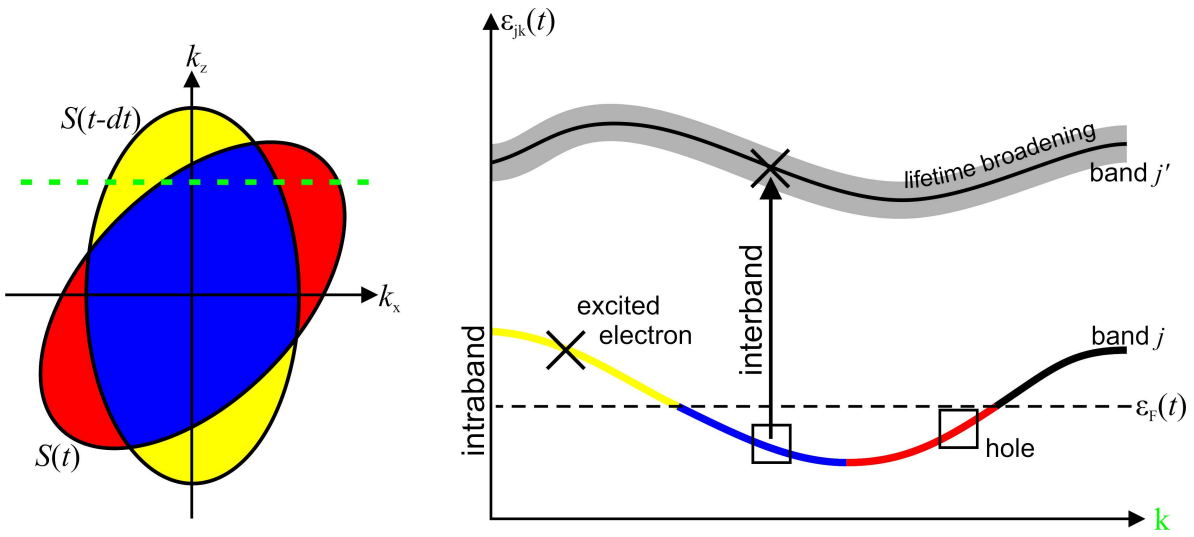


FIG. 1: A sketch of the adiabatic Fermi surface $S$ for time $t - \mathrm{d}t$ and time $t$ (Fig. 1a, left part). In a strictly adiabatic situation the yellow states are occupied only at time $t - \mathrm{d}t$, the red states are occupied only at time $t$, whereas the blue states are occupied at both times. Fig. 1b (right part) shows a sketch of the adiabatic bandstructure $\varepsilon_{j\mathbf{k}}(t)$ along the direction in k-space indicated by the horizontal dashed line in Fig. 1a. For a realistic situation where the $n_{j\mathbf{k}}$ lag behind the $f_{j\mathbf{k}}$ there may be some yellow states which should be empty in a strictly adiabatic situation but which are occupied in a realistic situation. Furthermore, there may be some red states which should be occupied but which are still empty. In Fig. 1b there is also a sketch for the interband transitions.

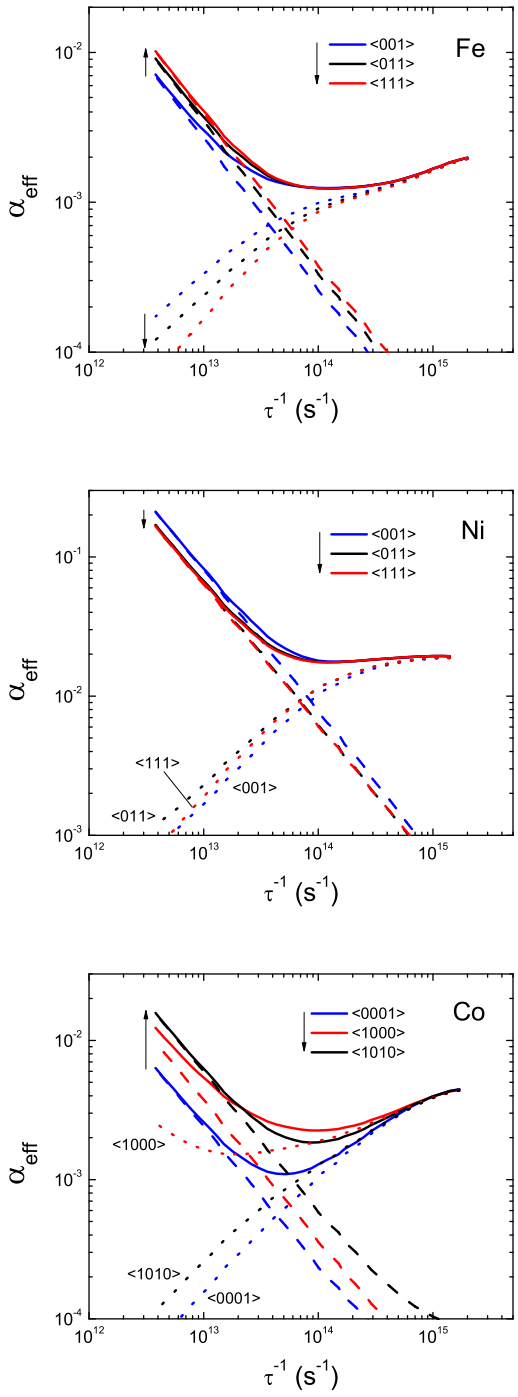


FIG. 2: The effective damping parameter $\alpha_{\rm eff}$ for Fe (top), Ni (middle) and Co (bottom) vs. electron scattering rate $\tau^{-1}$, for various orientations of the prescribed axis around which the small-angle precession of the magnetization vector takes place. Full lines: total damping, dashed lines: conductivity-like contribution, dotted lines: resistivity-like contribution.